

# Vehicular exhaust contributions to high NH<sub>3</sub> and PM<sub>2.5</sub> concentrations during winter in Tokyo, Japan

Kazuo Osada<sup>1</sup>, Shinji Saito<sup>2</sup>, Hiroshi Tsurumaru<sup>2</sup>, Junya Hoshi<sup>2</sup>

<sup>1</sup> GSES, Nagoya University, Furo-cho, Chikusa-ku, Nagoya 464-8601, Japan

5 <sup>2</sup> Tokyo Metropolitan Research Institute for Environmental Protection, Shinsuna 1-7-5, Koto-ku, Tokyo, 136-0075, Japan

*Correspondence to:* Kazuo Osada (kosada@nagoya-u.jp)

**Abstract.** Concentrations of PM<sub>2.5</sub> in Tokyo, a densely populated megacity, often increase because of NH<sub>4</sub>NO<sub>3</sub> formation under low-wind conditions during winter. To obtain source information of NH<sub>3</sub> as a NH<sub>4</sub>NO<sub>3</sub> precursor, hourly NH<sub>3</sub> and NH<sub>4</sub><sup>+</sup> concentrations were measured at an urban site in  
10 Tokyo in December 2017. Results show that PM<sub>2.5</sub> and NH<sub>4</sub><sup>+</sup> concentrations increased simultaneously under low-wind and low-temperature conditions along with NH<sub>3</sub>, NO<sub>x</sub>, CO, and optical black carbon (OBC) concentrations. The remaining NH<sub>4</sub><sup>+</sup> (herein, ΔNH<sub>4</sub><sup>+</sup>) subtracted from observed NH<sub>4</sub><sup>+</sup> to equivalent SO<sub>4</sub><sup>2-</sup> concentration correlated well with NO<sub>3</sub><sup>-</sup> in PM<sub>2.5</sub>, indicating the existence of fine  
15 NH<sub>4</sub>NO<sub>3</sub> particles. Regression analysis of hourly NH<sub>3</sub> + ΔNH<sub>4</sub><sup>+</sup> concentrations with CO, NO<sub>x</sub>, and OBC showed significant correlation. Virtual emission rates (VER) of NH<sub>3</sub> per motor vehicle in Tokyo were estimated using observed relations between NH<sub>3</sub> + ΔNH<sub>4</sub><sup>+</sup> and OBC, etc. with data from vehicular statistics: they were 3.7–32 mg/km. The regression of NH<sub>3</sub> + ΔNH<sub>4</sub><sup>+</sup> with OBC concentrations indicated an intercept of about 3.2 ppb, which is about half of the monthly average in  
20 December. This result implies that the non-vehicular source strength was nearly the same strength as the bulk vehicular emissions of NH<sub>3</sub> during winter in Tokyo.

Key words: hourly measurement, motor vehicle exhaust, NH<sub>3</sub>, urban source

Highlights:

- \* Considering excess NH<sub>4</sub><sup>+</sup> concentrations over SO<sub>4</sub><sup>2-</sup> was useful to study urban NH<sub>3</sub>.
- 25 \* Virtual emission rates of NH<sub>3</sub> per vehicle in Tokyo were 3.7–32 mg/km.
- \* Non-vehicular NH<sub>3</sub> sources contributed almost equally to winter vehicular emissions.

Published in [ATMOSPHERIC ENVIRONMENT, vol.206, 218-224, 2019](#)

## 1 Introduction

Ammonia ( $\text{NH}_3$ ) in the atmosphere plays an important role in various chemical, climatic, and environmental processes including neutralization of acidic substances (gases, particles, and droplets),  
35 formation of secondary aerosol particles, soil acidification, and water eutrophication (Behera et al., 2013; Seinfeld and Pandis, 2016). In fact, atmospheric  $\text{NH}_3$  has been recognized as the major precursor of fine particles such as ammonium sulfate and ammonium nitrate (Seinfeld and Pandis, 2016), which might affect human health, visibility, and the Earth's radiation balance. Wet and dry deposition of  $\text{NH}_3$  and particles containing ammonium salts to the Earth's surface might markedly  
40 alter the nitrogen cycle of natural ecosystem, engendering alteration of plant community composition, and causing other ill effects (Cape et al., 2009; Behera et al., 2013).

Various natural and anthropogenic sources emit  $\text{NH}_3$  (Sutton et al., 2008; Behera et al., 2013). Agriculture is the dominant source on a global scale, contributing more than 80% of global  $\text{NH}_3$  emissions. For urban areas, non-agricultural  $\text{NH}_3$  sources have been reported as major contributors to  
45 the concentration levels. They include emissions from related anthropogenic wastes (sewage disposal, etc.; Pandolfi et al., 2012; Reche et al., 2012, 2015), green spaces with plants and soils located in street canyons (Hu et al., 2014; Teng et al., 2017), and motor vehicles (e.g., Perrino et al., 2002; Cape et al., 2004; Li et al., 2006; Matsumoto et al., 2006; Nowak et al., 2006; Chang et al., 2016). Evaporation of  $\text{NH}_3$  from waste materials, plants, and soils is mainly related to pH and temperature:  
50 higher temperatures allow higher atmospheric concentrations, leading to diurnal flux and concentration variation synchronized with air temperature peaking near noon time (Roelle and Aneja, 2002; Kruit et al., 2007). Regarding emissions from motor vehicles, however, the emission strength (the number of active motor vehicles) in urban areas is expected to show large diurnal variation, with maximum concentrations occurring during the morning rush hour (Perrino et al., 2002; Li et al., 2006;  
55 Nowak et al., 2006).

To reduce CO, hydrocarbon, and  $\text{NO}_x$  emissions from gasoline-powered vehicles, three-way catalytic converters (TWC) have been widely introduced since the 1980s. When using the TWC, however,  $\text{NH}_3$  has been emitted as a side product in the  $\text{NO}_x$  reduction process, thereby contributing as an  $\text{NH}_3$  source in the urban atmosphere (e.g., Fraser and Cass, 1998; Kean et al., 2009). In addition,  
60 to reduce  $\text{NO}_x$  emission from heavy-duty and light-duty diesel powered vehicles, application of selective catalytic reduction (SCR) systems using urea started in the mid-2000s in Japan and later in other countries, often contributing even more  $\text{NH}_3$  to the atmosphere (Suzuki et al., 2008; Carslaw and Rhys-Tyler, 2013; Yamamoto et al., 2013; Suarez-Bertoa et al., 2016). Because of the short lifetime of ammonia in the atmosphere, the influence of even a strong point source such as a livestock  
65 facility is mostly limited to a few kilometers (Asman et al., 1989; Hojito et al., 2006; Shen et al.,

2016). Such agricultural facilities are usually absent from urban areas. Therefore, gasoline-powered and diesel-powered vehicles might be the dominant contributors of atmospheric NH<sub>3</sub> within urban areas.

In urban areas, air pollution episodes resulting from local emissions have often occurred during cold seasons (e.g., Kukkonen et al., 2005). Development of strong temperature inversion layers under low-wind conditions is responsible for many cases of heightened concentrations of pollutants such as NO<sub>x</sub> and PM<sub>2.5</sub>.

Tokyo is among the largest metropolitan areas in the world (The United Nations, 2016). In addition, Tokyo is among of the most densely populated megacities in the world (population density of about 6,200 persons km<sup>-2</sup> in 2015; <http://www.metro.tokyo.jp/ENGLISH/ABOUT/HISTORY/history03.htm>). In light of the high density of population, industries, and motor vehicles in megacities, air quality in Tokyo has often not been healthy, but it has improved gradually during recent decades (Minoura et al., 2006; Hara et al., 2013; Wakamatsu et al., 2013). Nevertheless, for particulate matter in Tokyo, high-PM<sub>2.5</sub> episodes with concentrations greater than the daily regulatory value in Japan still occur, especially in winter. Nitrate and ammonium have been reported as dominant ions in fine particles during such episodes, especially in winter (Minoura et al., 2006; Saito et al., 2012). To investigate the origin and cause of high PM<sub>2.5</sub> related to reactive nitrogen species, detailed time variation data of NH<sub>3</sub> and NH<sub>4</sub><sup>+</sup> must be obtained with other tracer species of motor vehicle exhaust. This report presents results of such observations conducted in December 2017 in Tokyo. These data are expected to elucidate ambient NH<sub>3</sub> levels, the relation with PM<sub>2.5</sub>, and their contributions to high-PM<sub>2.5</sub> events from vehicular emissions in this area. We also attempted to quantify annual NH<sub>3</sub> emissions from bulk vehicles in the Tokyo metropolitan area because of the importance of obtaining realistic data on the NH<sub>3</sub> budget in the urban atmosphere.

90

## 2 Observation

Gaseous NH<sub>3</sub> and NH<sub>4</sub><sup>+</sup> concentrations in fine particles were measured using a semi-continuous microflow analytical system (ANH-16; Kimoto Electric Co. Ltd.; Osada et al., 2011) at the sixth floor of the main building of Tokyo Metropolitan Research Institute for Environmental Protection (35.67°N, 139.83°E, Fig. 1) located in the southern Tokyo metropolitan area. Two identical sampling lines were used to differentiate total ammonium (NH<sub>3</sub> and NH<sub>4</sub><sup>+</sup>) and NH<sub>4</sub><sup>+</sup> alone using a H<sub>3</sub>PO<sub>4</sub> denuder to remove NH<sub>3</sub> from the sample air stream. An impactor having a 50% cut-off diameter at about 2 μm was installed at the inlet. The sample air was introduced into an inner frosted glass tube (3 mm inner diameter, 50 cm long) at a flow rate of 1 L min<sup>-1</sup>. One was coated inside by H<sub>3</sub>PO<sub>4</sub>. The

100 other was uncoated. After passage through the glass tube, water droplets were added to the sample air at  $100 \mu\text{l min}^{-1}$  and were mixed in a 5-m-long Teflon tube. The sample water was separated using an air–liquid separator and was injected into the microflow fluorescence analyzer to quantify the  $\text{NH}_4^+$  concentration (Osada et al., 2011; Osada et al., 2018). Analysis of the sample solution took 15 min. Consequently, the dataset of  $\text{NH}_4^+$  plus  $\text{NH}_3$  and  $\text{NH}_4^+$  alone was obtainable at 30 min intervals. 105 The detection limit of  $\text{NH}_3$  concentration was about 0.1 ppbv (Osada et al., 2011) under stable atmospheric  $\text{NH}_3$  and  $\text{NH}_4^+$  concentrations. Equivalence of two sample lines and the span of the calibration slope were checked periodically using  $\text{NH}_3$  standard gas at about 4 ppbv diluted from 100 ppmv (Taiyo Nippon Sanso Corp.). The ANH-16 was calibrated periodically with a standard  $\text{NH}_4^+$  solution prepared from a certified 1000 ppm solution (Fujifilm Wako Pure Chemical Corp.).

110 Just as  $\text{NO}$  and  $\text{NO}_x$  were measured (APNA-370; Horiba Ltd.),  $\text{CO}$  was measured (48i TLE; Thermo Fisher Scientific Inc.). We measured  $\text{PM}_{2.5}$  and optical black carbon (OBC, PM712; Kimoto Electric Co. Ltd.). Hourly concentrations of  $\text{NO}_3^-$  and  $\text{SO}_4^{2-}$  in  $\text{PM}_{2.5}$  were measured (ACSA-14; Kimoto Electric Co. Ltd., Saito et al., 2012). Measurement methods for  $\text{NO}_3^-$  and  $\text{SO}_4^{2-}$  used in ACSA-series were evaluated by Osada et al. (2016). For this study, we adjusted ACSA-based daily 115 mean values to daily mean values based on the reference method (Federal Reference Method, EPA, 1999), if necessary. Meteorological data were obtained at the Japan Meteorological Agency’s Tokyo regional headquarters, located about 6 km northwest of the site (JMA, 2018).

### 3 Results and Discussion

120 Figure 2 presents results of observations conducted in December 2017. In Tokyo, days of low wind speed were frequent in December, 2017. Indeed, the hours below  $3 \text{ m s}^{-1}$  were 543 out of 744 hr in December, comprising about 73% of the month. Because of low winds during winter, a surface inversion layer often developed, preventing the vertical diffusion of locally emitted pollutants. Therefore, atmospheric concentrations of  $\text{CO}$ , OBC, and  $\text{NO}_x$ , mainly emitted from automobile 125 exhausts, were often higher under low-wind conditions in winter. In Fig. 2, for example, the concentration peaks on December 7th–8th, 10th–11th, 15th–16th, 18th–19th, and 22nd–24th were associated with low winds. High  $\text{NO}_x$  correlates well with high  $\text{NO}$  concentrations, suggesting that emissions from internal combustion are the dominant source of  $\text{NO}_x$  enhancement. Moreover, the  $\text{NH}_3$  concentration increased under low winds. The similarity of  $\text{NH}_3$  temporal variation with those 130 of species emitted from motor vehicles suggests that  $\text{NH}_3$  was emitted from motor vehicles. Correlation between  $\text{NH}_3$  and vehicle-emitted species in the urban area has been reported for many cities (Perrino et al., 2002; Li et al., 2006; Nowak et al., 2006).

Figure 3 presents concentrations of  $\text{NH}_4^+$ ,  $\text{SO}_4^{2-}$ ,  $\text{NO}_3^-$ , and  $\Delta\text{NH}_4^+$  in  $\text{PM}_{2.5}$ . Concentrations of  $\text{SO}_4^{2-}$  were much lower than that of  $\text{NO}_3^-$  or  $\text{NH}_4^+$ . Actually, the  $\text{SO}_2$  concentrations (not shown) in Tokyo were also low (ca. 1 ppb; MOE, 2018a) in December. The oxidation speed of  $\text{SO}_2$  was expected to be low in winter. Therefore, the amount of in-situ formation of  $\text{SO}_4^{2-}$  from local  $\text{SO}_2$  oxidation is expected to be limited. Long-range transport of fine particles containing  $(\text{NH}_4)_2\text{SO}_4$  might contribute to  $\text{NH}_4^+$  to some degree in Tokyo. As Fig. 3 shows,  $\text{NH}_4^+$  resulting from such  $(\text{NH}_4)_2\text{SO}_4$  accounts for about 30% at most because of the low  $\text{SO}_4^{2-}$  concentrations observed during this period. Here we define  $\Delta\text{NH}_4^+$  concentrations as

$$[\Delta\text{NH}_4^+] = [\text{NH}_4^+] - [2 \text{SO}_4^{2-}] , \quad (1)$$

where  $[x]$  denotes the concentration of  $x$  species in nanomoles per cubic meter. The  $\Delta\text{NH}_4^+$  concentration indicates an extra amount of  $\text{NH}_4^+$  after subtracting the fully neutralized amount as forming  $(\text{NH}_4)_2\text{SO}_4$ . In other words, the amount of  $\text{NH}_4^+$  potentially existed as ammonium nitrate ( $\text{NH}_4\text{NO}_3$ ). Temporal variation of the  $\Delta\text{NH}_4^+$  correlates very well with  $\text{NO}_3^-$  concentrations, indicating that most of the  $\text{NO}_3^-$  existed as  $\text{NH}_4\text{NO}_3$ . A slightly higher  $\Delta\text{NH}_4^+$  concentration suggests potential on other counterpart anions (such as  $\text{Cl}^-$  and organic acids) to neutralize or slightly overestimating  $\text{NO}_3^-$  concentrations because of interference from water-soluble organics (Osada et al., 2016). As Fig. 2 shows,  $\text{NO}_x$  concentrations often exceeded 100 ppb, which can produce high levels of  $\text{N}_2\text{O}_5$  or  $\text{HNO}_3$ . High  $\text{NH}_3$  concentrations with  $\text{HNO}_3$  in the atmosphere promote  $\text{NH}_4\text{NO}_3$  formation, especially under cold temperatures (Mozurkewich, 1993). The mean air temperature in Tokyo was  $6.6^\circ\text{C}$  during December 2017 (Japan Meteorological Agency, 2018). According to monitoring data for acid-rain-related species by the Ministry of Environment in Japan (MOE, 2018a), the monthly average  $\text{HNO}_3$  concentration was about 0.3 ppb in December (2011–2016) in Tokyo. The mean  $\text{NH}_3$  concentration observed for this study was 4.1 ppb. On average, the concentration products of gaseous  $\text{NH}_3$  and  $\text{HNO}_3$  were higher (about a factor of 4) than the gas–solid equilibrium value for  $\text{NH}_4\text{NO}_3$  at  $6.6^\circ\text{C}$  based on parameters reported by Mozurkewich (1993). This result strongly suggests the frequent formation of  $\text{NH}_4\text{NO}_3$  in the atmosphere and an increasing contribution of  $\text{NH}_4\text{NO}_3$  to  $\text{PM}_{2.5}$  concentration, which is consistent with high  $\text{NH}_4\text{NO}_3$  fraction to  $\text{PM}_{2.5}$  under high  $\text{NO}_x$ ,  $\text{NH}_3$ , and low-wind conditions.

Sewage disposal plants are potential sources of urban  $\text{NH}_3$ . The nearest such plant, the Sunamachi sewage plant, is located 1 km southeast from the observation site. To detect any influence of plant emissions, hourly  $\text{NH}_3$  concentrations were taken by wind direction as a polar plot portrayed in Fig. 4. Higher  $\text{NH}_3$  concentrations were observed from west to north winds as opposed to the direction of the sewage plant. The area of north to west from the site is covered by densely populated metropolitan areas, whereas Tokyo Bay lies to the south (Fig. 1). Anthropogenic  $\text{NH}_3$  emissions such

as those from humans themselves, pets, sewage treatment, and garbage are known as major contributors to the urban atmosphere, especially during warm seasons (Reche et al., 2012). Our study was conducted in winter. Therefore, emission flux from these sources is limited because of the prevailing low temperatures. Reche et al. (2012) pointed out that the number of garbage containers per unit of area affects the local  $\text{NH}_3$  concentration in Barcelona. However, domestic waste collection in Japan generally requires 1) that burnable waste including food waste, etc. be packed into plastic bags and 2) that stringent rules be applied for public collection (e.g., garbage bags must be put out in a specified collection place by 8:00 a.m. on the collection day), preventing unnecessary  $\text{NH}_3$  emissions during garbage collection.

For polar plots on  $\text{NO}_x$ , OBC, and CO, higher concentrations were also observed for west to north winds, implying that motor vehicle emissions from metropolitan areas are greater than those from the Tokyo Bay area. The similarity of higher directions for these with  $\text{NH}_3$  suggests that, for  $\text{NH}_3$  in winter, motor vehicle exhausts are potentially the major contributor at the site, rather than sewage plant emissions.

Figure 5 portrays scatter plots of  $\text{NH}_3 + \Delta\text{NH}_4^+$  among hourly concentrations for vehicular exhaust markers in December 2017. All panels in Fig. 5 depict significant correlation at a 99% confidence level ( $n=663$ ). Regarding conversion of concentrations from OBC to elemental carbon (EC), daily relations between those at Nagoya were used (Osada et al., 2019). The EC concentrations were estimated as OBC concentrations multiplied by 1.25. They are expressed as mole fractions (ppb) in the air for comparative purposes. A higher coefficient of determination ( $R^2 > 0.8$ ) was obtained for pairs of vehicular marker species (EC, CO, and  $\text{NO}_x$ ). The  $R^2$  (0.48) between  $\text{NO}_x$  and  $\text{NH}_3 + \Delta\text{NH}_4^+$  was higher than that (0.36) for the relation between  $\text{NH}_3$  and  $\text{NO}_x$ , suggesting that the concentration of  $\text{NH}_3 + \Delta\text{NH}_4^+$  is useful to study the  $\text{NH}_3$  budget considering  $\text{NH}_4\text{NO}_3$  formation in the atmosphere. The highest  $R^2$  found for  $\text{NH}_3 + \Delta\text{NH}_4^+$  was obtained for OBC (0.60). As the panel shows, the intercept of the regression line for  $\text{NH}_3 + \Delta\text{NH}_4^+$  with OBC is about 3.2 ppb, which suggests the existence of a non-vehicular source for  $\text{NH}_3$ . The monthly average of  $\text{NH}_3 + \Delta\text{NH}_4^+$  was 6.7 ppb. Therefore, the non-vehicular source contribution accounts for about 48% of the average. In turn, vehicular emissions contribute to about half of the average concentration of  $\text{NH}_3 + \Delta\text{NH}_4^+$  in December.

Table 1 presents annual emission amounts of the vehicular markers in Tokyo and slope values of regression analysis in Fig. 5. Vehicular emissions were taken from the latest report for 2015 (Bureau of Environment Tokyo Metropolitan Government, 2017). The report, which has been compiled every five years, is based on various chassis dynamometer experiments and traffic surveys in Tokyo. The emission amount of EC was estimated as 70% of particle emissions from vehicular exhausts (Hagino

et al., 2010; Yamagami et al., 2019). Based on these emissions and observed slopes, annual emission amounts of  $\text{NH}_3$  from motor vehicles are estimated. For example, because the slope value on  $(\text{NH}_3 + \Delta\text{NH}_4^+)/\text{OBC}$  (EC) and EC emissions are, respectively, 1.46 and 69 ton/yr, proportional  $\text{NH}_3$  emissions are calculated as 143 ton/yr. Similarly, data based on CO and  $\text{NO}_x$  respectively provide 456 and 1245 ton/yr. Actually,  $\text{NH}_3$  emissions based on the slope with  $\text{NO}_x$  were much larger than others. The accuracy of these estimates depends on the correctness of emissions inferred from vehicular emission markers and regression slopes. Other than these sources of uncertainty, larger estimates based on  $\text{NO}_x$  might be attributed to one or more of the following: 1) low emissions for 2017 than those compiled for 2015 and 2) rapid oxidation of  $\text{NO}_x$  and efficient removal from the atmosphere. First, emission controls of  $\text{NO}_x$  for new vehicles in Japan have strengthened for these years, especially for diesel heavy vehicles (from 2.0 g/kWh in 2005 to 0.7 g/kWh at 2009, 0.4 g/kWh in 2016; MOE, 2018b). According to the latest report for 2015 (Bureau of Environment Tokyo Metropolitan Government, 2017),  $\text{NO}_x$  emission factors (EFs) estimated for passenger and freight vehicles decreased respectively about 56% and 24% during 2010–2015. Older high-emission vehicles are gradually being replaced by newer and lower emission vehicles. Therefore, the decreasing trend of EF continues from 2015 through 2017. Second, regarding behavior in the atmosphere, atmospheric residence time is about two months for CO and more than several days for fine particles, representing about OBC (Warneck, 2000). In contrast,  $\text{NO}_x$  is unstable in the atmosphere because of its rapid oxidation. In fact, the  $\text{NO}_x$  lifetime has been estimated to be as short as 8 hr, even in winter (Beirle et al., 2011), which is much shorter than that of either CO or OBC. Therefore, the observed slope to  $\text{NO}_x$  might be overestimated; consequently,  $\text{NH}_3$  emissions might be overestimated.

As shown in Table 1, virtual emission rates (VERs) of  $\text{NH}_3$  per motor vehicles in Tokyo were also estimated as annual emission amounts divided by the running number of vehicles and road distance in 2015. The value of traffic surveys was taken from a report by the Bureau of Environment Tokyo Metropolitan Government (2017). The VER estimation results show large dispersion (3.7–32), which is likely to be attributable to the reasons described above. Table 2 presents the VER obtained in this study and EFs from other studies obtained using various methods and at various places. Although the VER calculation method differs from EFs based on direct observations on single or many sample vehicles, comparison of these values is useful to elucidate bulk emissions from motor vehicles in an area. The EF data presented in Table 2 were selected from recent (after 2009) published data because of the rapid evolution of emissions control technologies worldwide. The range of the VERs obtained in this study is within the range of reported values. Actually,  $\text{NH}_3$  EFs have been estimated from observations at tunnels and measurements of chassis dynamometers, both of which are expensive and which require much equipment. In contrast, once hourly relations of  $\text{NH}_3 + \Delta\text{NH}_4^+$

235 with vehicular markers and their areal emission strengths in an area are available. Our method might be useful to estimate  $\text{NH}_3$  emission rates for bulk motor vehicle activities in the area.

In Japan, implementation of the SCR system using urea started for heavy-duty trucks and other vehicles after the mid-2000s. An older SCR system in use might produce more  $\text{NH}_3$  (Suzuki et al., 2008; 2014; Carslaw and Rhys-Tyler, 2013) and would enhance the EF of  $\text{NH}_3$  from diesel vehicles.  
240 Further simultaneous observations of  $\text{NH}_3 + \Delta\text{NH}_4^+$  and vehicular exhaust markers must be conducted to estimate VERs for  $\text{NH}_3$  more precisely across urban areas.

As discussed earlier, the intercept of the regression line suggests that non-vehicular sources accounted for about half the monthly average. The wide scatter shown in the plot between  $\text{NH}_3 + \Delta\text{NH}_4^+$  and vehicular markers suggests that the non-vehicular source strength might vary with  
245 parameters other than vehicular rush and vertical mixing. Using the regression results with OBC, the residual concentration (observed minus estimated) of  $\text{NH}_3 + \Delta\text{NH}_4^+$  is shown with air temperature in Fig. 6. Some larger positive deviations marked by asterisks are found for days of higher daytime temperature. Furthermore, detailed examination indicates that the daily peak of the residual value was found before the maximum of air temperature but after the morning. This indication suggests that the  
250 variation of residual  $\text{NH}_3 + \Delta\text{NH}_4^+$  resulted not only from air temperature but also because of other parameters. Dissociation of  $\text{NH}_4\text{NO}_3$  under higher temperatures has already been regarded as the use of  $\text{NH}_3 + \Delta\text{NH}_4^+$ . Evaporation of dew has been implicated as a cause of morning  $\text{NH}_3$  peak from grassland areas (Wenworth et al., 2014; 2016) and building walls (Osada et al., 2018). Prior deposition of  $\text{NH}_4^+$  species with water (dew, fog, etc.) during the nighttime under high relative  
255 humidity is a key process promoting morning evaporation. According to Wenworth et al. (2014 and 2016), higher morning  $\text{NH}_3$  peaks were observed after higher relative humidity (>90%) during the previous nighttime. However, nighttime relative humidity did not reach such high values in this study, mostly around 70% except for the early morning of December 5. This finding implies that dew evaporation might not be the major cause at these events. Teng et al. (2017) reported that emissions  
260 from urban soils in green space likely caused the spikes of atmospheric  $\text{NH}_3$  occurring 1–4 hr after morning rush hours. Such timing of morning peak after morning rush hours accords with results of this study. Relations with air temperature also partly support emanation from soil. However, areas of green space around the observation site are few. Moreover, input of  $\text{NH}_4^+$  species to soil surface, such as wet deposition of  $\text{NH}_4^+$ , was slight during this study: rain was observed only on December 8 and  
265 25. Given these limitations, although soil emissions at green space might be a possible urban  $\text{NH}_3$  source, it might not be sufficient to provide the  $\text{NH}_3$  peaks that require similar or greater magnitudes larger than those of vehicular emissions of 143 ton/yr or more.

## 270 4 Summary and Conclusions

Simultaneous and continuous measurements of gaseous  $\text{NH}_3$  and  $\text{NH}_4^+$  in fine particles were conducted at an urban site in Tokyo in December 2017. Together with results found for  $\text{PM}_{2.5}$ ,  $\text{NO}_x$ , CO, and OBC concentrations, both  $\text{NH}_3$  and  $\text{NH}_4^+$  concentrations were increased simultaneously under low-wind conditions. Analyses of  $\text{NO}_3^-$  and  $\text{SO}_4^{2-}$  in  $\text{PM}_{2.5}$  with  $\text{NH}_4^+$  indicated that residual  
275 amounts (defined as  $\Delta\text{NH}_4^+$ ) subtracted for equivalent concentration of  $\text{SO}_4^{2-}$  from observed  $\text{NH}_4^+$  concentrations correlated well with  $\text{NO}_3^-$ , suggesting the formation of  $\text{NH}_4\text{NO}_3$  in the atmosphere. Considering the high fraction of particulate  $\text{NH}_4\text{NO}_3$ , vehicular emissions of both  $\text{NO}_x$  and  $\text{NH}_3$  contribute to high  $\text{PM}_{2.5}$  events during winter in metropolitan Tokyo.

Several analyses were conducted to elucidate  $\text{NH}_3$  source contributions. Based on the polar plot  
280 of hourly  $\text{NH}_3$  concentrations by wind direction, the  $\text{NH}_3$  concentration from densely populated areas is higher than that from a local sewage plant. Regression analysis of hourly  $\text{NH}_3 + \Delta\text{NH}_4^+$  concentrations with vehicular exhaust markers (CO,  $\text{NO}_x$ , and OBC) showed significant correlation. Annual  $\text{NH}_3$  emission amounts from bulk (gasoline and diesel) vehicles in Tokyo were estimated using the regression slope and vehicular emission of CO,  $\text{NO}_x$ , and OBC. Furthermore, the virtual  
285 emission rate (VER) of  $\text{NH}_3$  per vehicle in Tokyo was calculated from running numbers of vehicles and road distances in 2015. The VER was 3.7–32 mg/km, which is within the range of recently reported emission factors based on measurements taken at tunnels and chassis dynamometers. The regression of  $\text{NH}_3 + \Delta\text{NH}_4^+$  concentrations with OBC indicated the intercept as about 3.2 ppb, which is about half of the monthly average in December. This indication implies that non-vehicular sources  
290 are nearly the same strength as the vehicular emission of  $\text{NH}_3$ . Non-vehicular and time-variable sources were discussed including soil emissions from green spaces.

Because of frequent calm wind conditions during winter at Tokyo, regression analysis of hourly data of  $\text{NH}_3$  and  $\text{NH}_4^+$  together with  $\text{PM}_{2.5}$ ,  $\text{NO}_x$ , CO, and OBC concentrations provide clues to separate vehicular and non-vehicular contribution of  $\text{NH}_3$ . Although plausible non-vehicular sources  
295 varying with temperature in winter were not specified, similar observations at multiple sites across an urban area might provide more clues revealing urban non-vehicular sources.

## 5 Acknowledgments

This research was supported by the Environment Research and Technology Development Fund  
300 (5-1604) of the Environmental Restoration and Conservation Agency.

## References

- Asman W.A., Pinksterboer E.F., Maas H.F., Erisman J.W., Waijers-Ypelaan A., Slanina J., Horst T.W., 1989. Gradients of the Ammonia Concentration in a Nature Reserve: Model Results and Measurements. *Atmos. Environ.* 23, 2259–2265.
- 305 Behera S.N., Sharma M., Aneja V.P., Balasubramanian R., 2013. Ammonia in the atmosphere: a review on emission sources, atmospheric chemistry and deposition on terrestrial bodies. *Environmental Science and Pollution Research International* 20, 8092–8131.
- Beirle, S., Boersma, K. F., Platt, U., Lawrence, M. G., & Wagner, T., 2011. Megacity emissions and lifetimes of nitrogen oxides probed from space. *Science* 333(6050), 1737–1739.
- 310 Bureau of Environment Tokyo Metropolitan Government, 2017. Report on emissions from vehicular exhausts in fiscal year 2015, 213p (in Japanese).
- Cape J.N., Tang Y.S., Van Dijk, N., Love L., Sutton M.A., Palmer S.C.F., 2004. Concentrations of ammonia and nitrogen dioxide at roadside verges, and their contribution to nitrogen deposition. *Environmental Pollution* 132(3), 469–478.
- 315 Cape J.N., van der Eerden L.J., Sheppard L.J., Leith I.D., Sutton M.A., 2009. Evidence for changing the critical level for ammonia. *Environmental Pollution* 157, 1033–1037.
- Carslaw D.C., Rhys-Tyler G., 2013. New insights from comprehensive on-road measurements of NO<sub>x</sub>, NO<sub>2</sub> and NH<sub>3</sub> from vehicle emission remote sensing in London, UK. *Atmospheric Environment* 81, 339–347.
- 320 Chang Y., Zou Z., Deng C., Huang K., Collett J. L., Lin J., Zhuang G., 2016. The importance of vehicle emissions as a source of atmospheric ammonia in the megacity of Shanghai. *Atmos. Chem. Phys.* 16, 3577–3594, doi:10.5194/acp-16-3577-2016.
- EPA, Federal Reference Method, 1999, <https://www3.epa.gov/ttnamti1/pmfrm.html>, last accessed on September, 25, 2018.
- 325 Fraser M.P., Cass G.R., 1998. Detection of excess ammonia emissions from in-use vehicles and the implications for fine particle control. *Environmental Science & Technology* 32(8), 1053–1057.
- Hagino, H., Sasaki, S., Nakayama, A., Nakajima, T., 2010. Organic carbon/elemental carbon emissions and their characterization from diesel engines and light-duty gasoline vehicles. *JARI Research Journal* 32 (12), 705–708 (in Japanese).
- 330 Hara K., Homma J., Tamura K., Inoue M., Karita K., Yano E., 2013. Decreasing trends of suspended particulate matter and PM<sub>2.5</sub> concentrations in Tokyo, 1990–2010. *Journal of the Air & Waste Management Association* 63(6), 737–748.

- Hojito M., Hayashi K., Murano K., Mori A., 2006. The Status of Atmospheric Concentrations of Ammonia in an Intensive Dairy Farming Area in Central Japan. *Japanese J. Soil Sci. Plant Nutrition* 77, 53–57 (in Japanese).
- 335
- Hu Q., Zhang L., Evans G.J., Yao X., 2014. Variability of atmospheric ammonia related to potential emission sources in downtown Toronto, Canada. *Atmospheric Environment* 99, 365–373.
- Japan Meteorological Agency, 2018, <http://www.jma.go.jp/jma/index.html>, last accessed on September 22, 2018
- 340 Kean A.J., Littlejohn D., Ban-Weiss G.A., Harley R.A., Kirchstetter T.W., Lunden M.M., 2009. Trends in on-road vehicle emissions of ammonia. *Atmospheric Environment* 43(8), 1565–1570.
- Kruit R.R.W., Van Pul W.A.J., Otjes R.P., Hofschreuder P., Jacobs A.F.G., Holtslag, A.A.M., 2007. Ammonia Fluxes and Derived Canopy Compensation Points over non-Fertilized Agricultural Grassland in The Netherlands Using the New Gradient Ammonia – High Accuracy – monitor (GRAHAM). *Atmos. Environ.* 41, 1275–1287.
- 345
- Kukkonen J., Pohjola M., Sokhi R.S., Luhana L., Kitwiroon N., Fragkou L., Denby B., 2005. Analysis and evaluation of selected local-scale PM10 air pollution episodes in four European cities: Helsinki, London, Milan and Oslo. *Atmospheric Environment* 39(15), 2759–2773.
- Li Y., Schwab J.J., Demerjian K.L., 2006. Measurements of Ambient Ammonia using a Tunable Diode Laser Absorption Spectrometer: Characteristics of Ambient Ammonia Emissions in an Urban Area of New York City, *J. Geophys. Res.* 111, D10S02, doi:10.1029/2005JD006275.
- 350
- Liu T., Wang X., Wang B., Ding X., Deng W., Lü S., Zhang Y., 2014. Emission factor of ammonia (NH<sub>3</sub>) from on-road vehicles in China: tunnel tests in urban Guangzhou. *Environ. Res. Lett.* 9(6), 064027.
- 355
- Livingston C., Rieger P., Winer A., 2009. Ammonia emissions from a representative in-use fleet of light and medium-duty vehicles in the California South Coast Air Basin. *Atmospheric Environment* 43(21), 3326-3333.
- Matsumoto R., Umezawa N., Karaushi M., Yonemochi S.I., Sakamoto K., 2006. Comparison of ammonium deposition flux at roadside and at an agricultural area for long-term monitoring: emission of ammonia from vehicles. *Water, Air, and Soil Pollution* 173(1–4), 355–371.
- 360
- Minoura H., Takahashi K., Chow J.C., Watson, J.G., 2006. Multi-year trend in fine and coarse particle mass, carbon, and ions in downtown Tokyo, Japan. *Atmospheric Environment* 40(14), 2478–2487.
- Ministry of Environment, 2018a. Monitoring data on acid rain for 2016, <https://www.env.go.jp/air/acidrain/>, last accessed on September 22, 2018.
- 365
- Ministry of Environment, 2018b. Regulation of motor vehicle exhaust, [https://www.env.go.jp/air/car/gas\\_kisei.html](https://www.env.go.jp/air/car/gas_kisei.html), last accessed on September 22, 2018.

- Mozurkewich M., 1993. The Dissociation Constant of Ammonium Nitrate and its Dependence on Temperature, Relative Humidity and Particle Size. *Atmos. Environ.* 27A, 261–270.
- Nowak J.B., Huey L.G. Russell A.G. Tian D. Neuman J.A. Orsini D. Sjostedt S.J. Sullivan A.P.  
370 Tanner D.J. Weber R.J. Nenes A. Edgerton E. Fehsenfeld F.C., 2006. Analysis of Urban Gas Phase Ammonia Measurements from the 2002 Atlanta Aerosol Nucleation and Real-Time Characterization Experiment (ANARChE). *J. Geophys. Res.* 111, D17308, doi:10.1029/2006JD007113.
- Osada K., Ueda S., Egashira T., Takami A., Kaneyasu N., 2011. Measurement of gaseous NH<sub>3</sub> and  
375 particulate NH<sub>4</sub><sup>+</sup> in the atmosphere by fluorescent detection after continuous air–water droplet sampling. *Aerosol and Air Quality Research* 11, 170–178.
- Osada K., Kamiguchi Y., Yamamoto S., Kuwahara S., Pan X., Hara Y., Uno I., 2016. Comparison of Ionic Concentrations on Size-Segregated Atmospheric Aerosol Particles Based on a Denuder-Filter Method and a Continuous Dichotomous Aerosol Chemical Speciation Analyzer (ACSA-12).  
380 *Eurozoru Kenkyu* 203–209, doi.org/10.11203/jar.31.203 (in Japanese).
- Osada K., Yamagami M., Ikemori F., Hisatsune K., Nakashima H., Miwa A., Yabutani S., 2018. Sudden increase in atmospheric NH<sub>3</sub> concentration after drying hydrometeor. *J. Jpn. Soc. Atmos. Environ.* 53(4), 130–135 (in Japanese).
- Osada, K., Yamagami, M., Hisatsune, K., Ikemori, F., Chatani, S., 2019. Sources of Optical Black  
385 Carbon at Nagoya Bay Area: Analysis under sea breeze condition. *J. Jpn. Soc. Atmos. Environ.* 54(2), in press (in Japanese).
- Pandolfi M., Amato F., Reche C., Alastuey A., Otjes R.P., Blom M.J., Querol X., 2012. Summer ammonia measurements in a densely populated Mediterranean city. *Atmospheric Chemistry and Physics* 12(16), 7557–7575.
- 390 Perrino C., Catrambone M.D., Di Bucchianico A.D.M., Allegrini I., 2002. Gaseous ammonia in the urban area of Rome, Italy and its relationship with traffic emissions. *Atmospheric Environment* 36, 5385–5394.
- Reche C., Viana M., Karanasiou A., Cusack M., Alastuey A., Artiñano B., de la Campa A.M.S., 2015. Urban NH<sub>3</sub> levels and sources in six major Spanish cities. *Chemosphere* 119, 769–777.
- 395 Reche C., Viana M., Pandolfi M., Alastuey A., Moreno T., Amato F., Querol X., 2012. Urban NH<sub>3</sub> levels and sources in a Mediterranean environment. *Atmospheric Environment* 57, 153–164.
- Roelle P.A., Aneja V.P., 2002. Characterization of ammonia emissions from soils in the upper coastal plain, North Carolina. *Atmospheric Environment* 36, 1087–1097.
- Saito S., Ishii K., Ueno H., Uchida Y., 2012. Chemical characteristics of principal PM<sub>2.5</sub> species in  
400 Tokyo Metropolitan: A case study. *Annual Report of Tokyo Metropolitan Research Institute for Environmental Protection*, 31–36 (in Japanese).

- Seinfeld J.H., Pandis S.N., 2016. Atmospheric chemistry and physics: from air pollution to climate change. John Wiley & Sons.
- Shen J., Chen D., Bai M., Sun J., Coates T., Lam S.K., Li Y., 2016. Ammonia deposition in the  
405 neighbourhood of an intensive cattle feedlot in Victoria, Australia. *Scientific Reports* 6, 32793.
- Suarez-Bertoa R., Mendoza-Villafuerte P., Bonnel P., Lilova V., Hill L., Perujo A., Astorga C., 2016. On-road measurement of NH<sub>3</sub> and N<sub>2</sub>O emissions from a Euro V heavy-duty vehicle. *Atmospheric Environment* 139, 167–175.
- Suarez-Bertoa R., Mendoza-Villafuerte P., Riccobono F., Vojtisek M., Pechout M., Perujo A.,  
410 Astorga C., 2017. On-road measurement of NH<sub>3</sub> emissions from gasoline and diesel passenger cars during real world driving conditions. *Atmospheric Environment* 166, 488–497.
- Suarez-Bertoa R., Zardini A.A., Astorga C., 2014. Ammonia exhaust emissions from spark ignition vehicles over the New European Driving Cycle. *Atmospheric Environment* 97, 43–53.
- Sutton M.A., Erisman J.W., Dentener F., Möller D., 2008. Ammonia in the environment: from ancient  
415 times to the present. *Environmental Pollution* 156(3), 583–604.
- Suzuki H., Ishii H., Sakai K., Fujimori K., 2008. Regulated and unregulated emission components characteristics of urea SCR vehicles. *Transactions of Society of Automotive Engineers of Japan* 39, 161–166 (in Japanese).
- Suzuki H., Yamamoto, T., Yamaguchi, K., 2014. Emission characteristic trends of in-use urea SCR  
420 HD vehicles. *Transactions of Society of Automotive Engineers of Japan* 45, 43–48 (in Japanese).
- Teng, X., Hu, Q., Zhang, L., Qi, J., Shi, J., Xie, H., Gao H., Yao, X., 2017. Identification of major sources of atmospheric NH<sub>3</sub> in an urban environment in northern China during wintertime. *Environ. Sci. Technol.* 51(12), 6839–6848.
- The United Nations, 2016. *The World's Cities in 2016*, 11p.
- 425 Vieira-Filho M.S., Ito D.T., Pedrotti J.J., Coelho L.H., Fornaro A., 2016. Gas-phase ammonia and water-soluble ions in particulate matter analysis in an urban vehicular tunnel. *Environmental Science and Pollution Research* 23(19), 19876–19886.
- Wakamatsu S., Morikawa T., Ito A., 2013. Air pollution trends in Japan between 1970 and 2012 and impact of urban air pollution countermeasures. *Asian Journal of Atmospheric Environment* 7(4),  
430 177–190.
- Warneck, P. 2000. *Chemistry of the Natural Atmosphere*. Second Edition. Academic Press Inc., San Diego, pp. 927.
- Wentworth, G. R., Murphy, J. G., Gregoire, P. K., Cheyne, C. A. L., Tevlin, A. G., Hems, R., 2014. Soil–atmosphere exchange of ammonia in a non-fertilized grassland: Measured emission  
435 potentials and inferred fluxes. *Biogeosciences* 11, 5675–5686.

Wentworth, G. R., Murphy, J. G., Benedict, K. B., Bangs, E. J., Collett Jr., J. L., 2016. The role of dew as a night-time reservoir and morning source for atmospheric ammonia. *Atmos. Chem. Phys.* 16, 7435–7449.

440 Yamagami, M., Ikemori, F., Nakashima, H., Hisatsune, K., Osada, K., 2019. Decreasing trend of elemental carbon concentration with changes in major sources at Mega city Nagoya. Central Japan, *Atmos. Environ.* 199, 155–163.

Yamamoto T., Tsutsumi R., Iwata T., Ogawa Y., Kato Y., 2013. Emission behaviour of NO<sub>x</sub>, NH<sub>3</sub> and N<sub>2</sub>O from the Truck equipped with urea SCR system under road driving. *Transactions of Society of Automotive Engineers of Japan* 44, 1489–1496 (in Japanese).

445

Table 1 Vehicular emissions in Tokyo at 2015, slope of regression analysis, vehicular emissions of NH<sub>3</sub> and virtual emission rates of NH<sub>3</sub>.

450	CO	NO <sub>x</sub>	EC
Emissions (ton/yr)*	32,588	17,297	69
455	slope to CO	slope to NO <sub>x</sub>	slope to EC (OBCx1.25)
NH <sub>3</sub> +ΔNH <sub>4</sub> <sup>+</sup>	0.014 (0.55)	0.072 (0.48)	1.46 (0.60)
460	from CO	from NO <sub>x</sub>	from EC (OBCx1.25)
Vehicular NH <sub>3</sub> # (ton/yr)	456	1,245	143
Virtual Emission Rate <sup>\$</sup> of NH <sub>3</sub> (mg/km)	12	32	3.7

\*: Bureau of Environment Tokyo Metropolitan Government, 2017

465 Slopes are calculated using mol units.

Numbers in parentheses denote coefficients of determination.

#: estimated for Tokyo as emissions multiplied in 2015 by the slope observed.

\$: estimated as NH<sub>3</sub> emissions divided by the number of running vehicles and distance (39,122 million vehicles•km) in Tokyo, 2015 (Bureau of Environment Tokyo Metropolitan Government, 2017).

470

475 Table 2 Virtual emission rate (VER) and emission factors (EFs) of NH<sub>3</sub> reported after 2009

Method	Location	VER (mg/km) EF (mg/km)	Reference
Regression analysis	Tokyo	3.7–32	this study
480 tunnel	Shanghai	28	Chang et al. (2016)
tunnel	São Paulo	44	Vieira-Filho et al. (2016)
tunnel	Guangzhou	230	Liu et al. (2014)
tunnel	California	49	Kean et al. (2009)
chassis dynamometer	Italy	2–8 (on-road)	Suarez-Bertoa et al. (2017)
485		45–134 (cold start)	
chassis dynamometer	Italy	4–70	Suarez-Bertoa et al. (2014)
chassis dynamometer	California	46	Livingston et al. (2009)

490

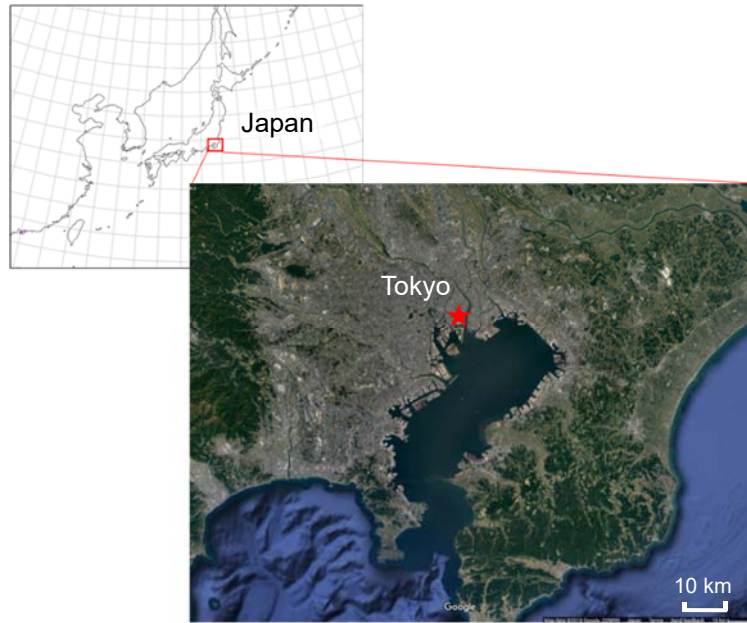


Figure 1 Map showing observation site (red asterisk,  $35.67^{\circ}\text{N}$ ,  $139.83^{\circ}\text{E}$ ) in Tokyo, Japan.

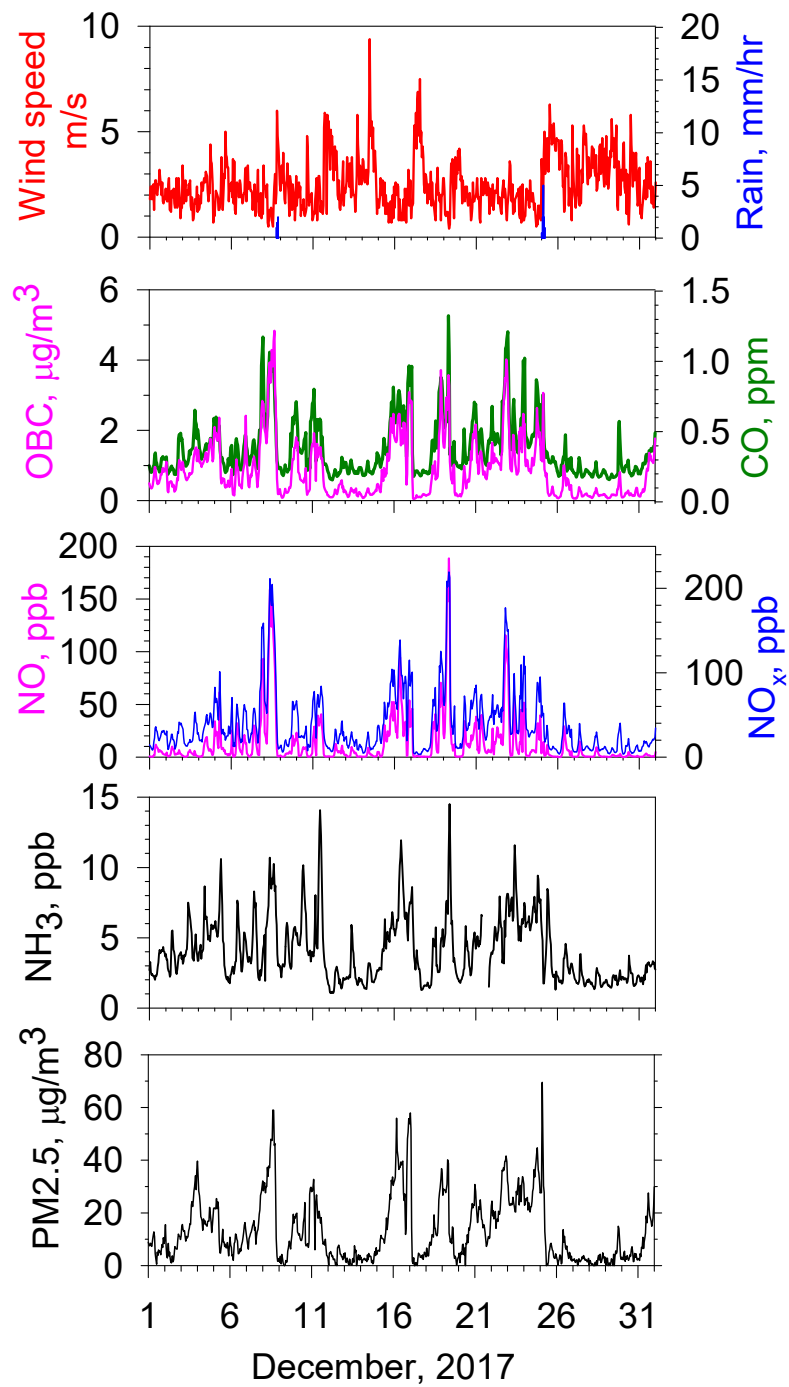


Figure 2 Observation results obtained in Tokyo during December, 2017. Meteorological data are from the Japan Meteorological Agency. OBC represents optical black carbon.

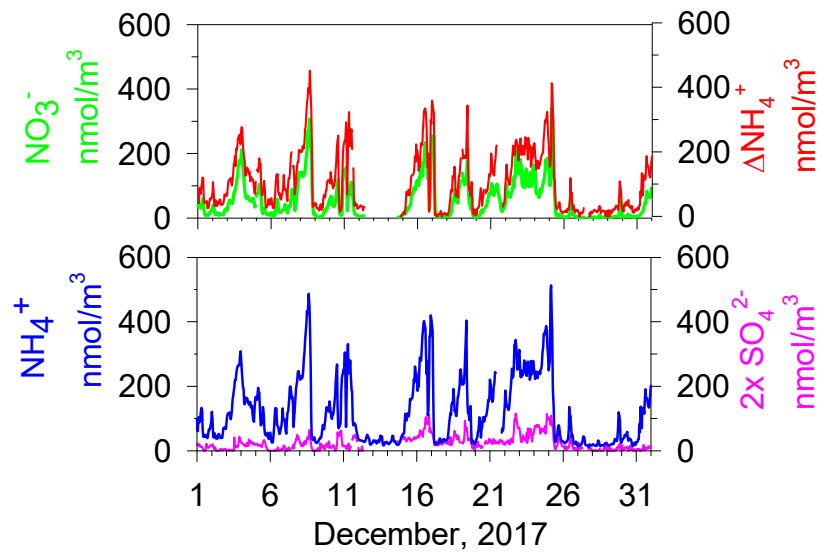


Figure 3 Ionic concentrations of  $\text{PM}_{2.5}$  in December, 2017.  $\Delta\text{NH}_4^+$  concentration represents  $[\text{NH}_4^+]$  minus  $2 \times [\text{SO}_4^{2-}]$  in nanomoles per cubic meter.

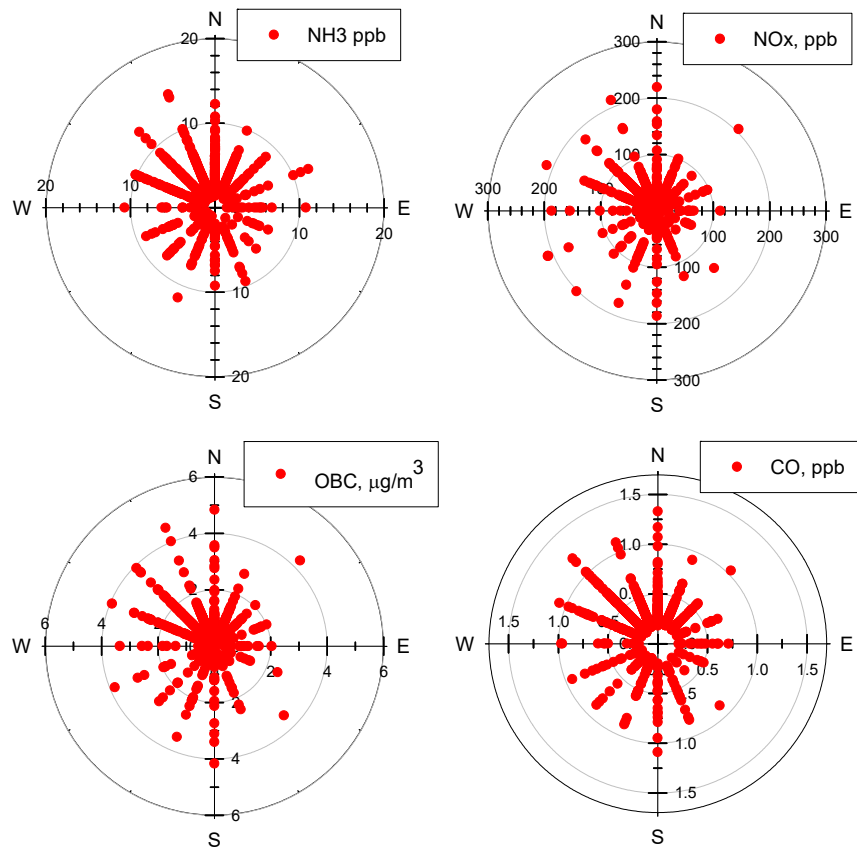


Figure 4 Polar plots of hourly concentrations by wind direction for December, 2017.

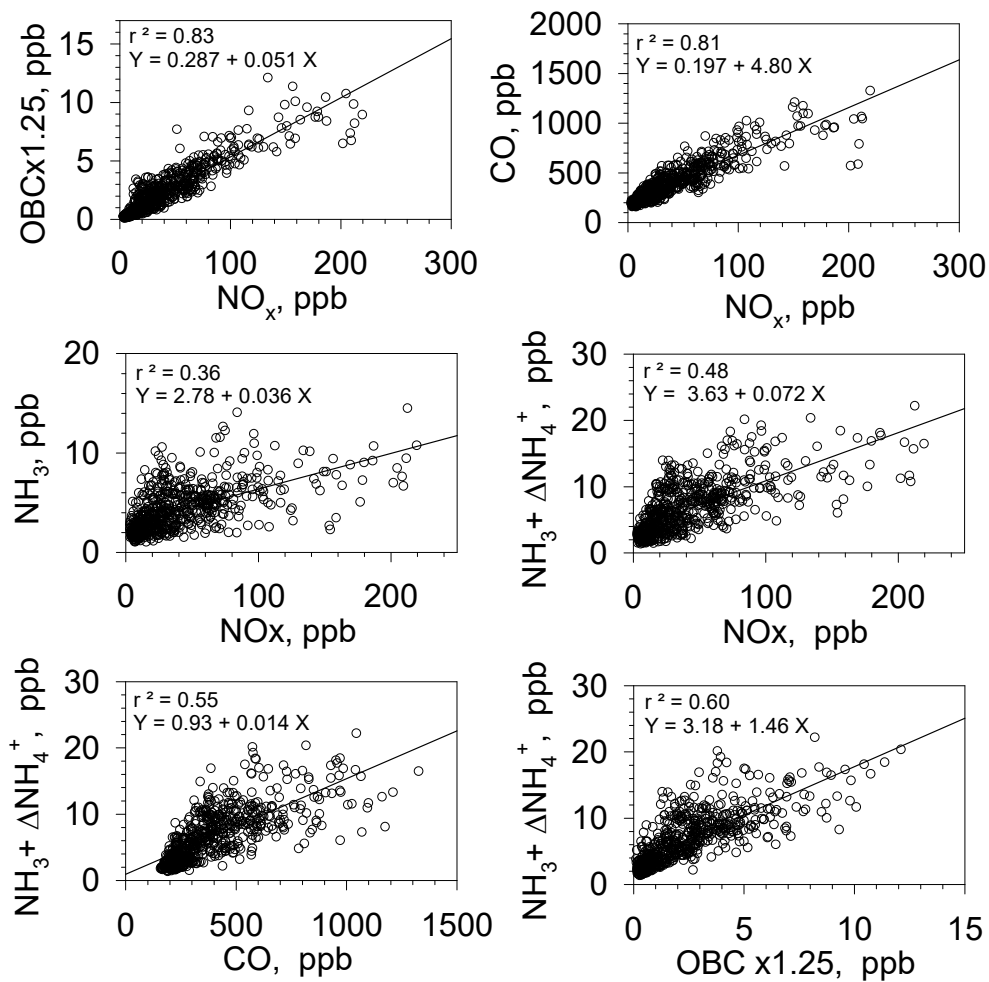


Figure 5 Scatter plots of hourly concentrations in December, 2017. Regression line, equation, and coefficient of determination are also presented in the panels.

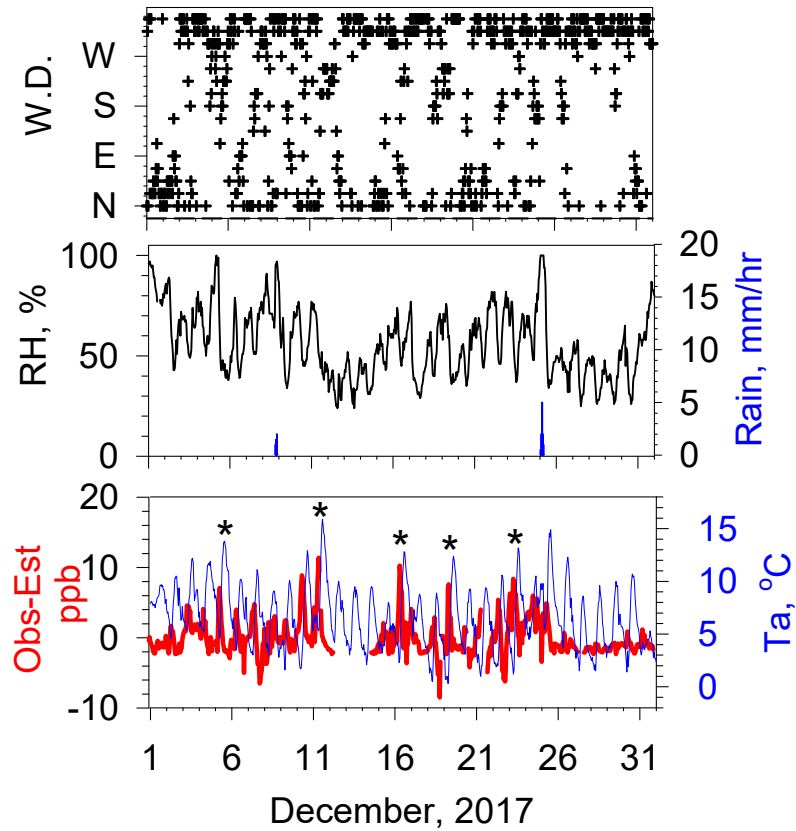


Figure 6 Upper panel: Wind direction. Middle panel: Relative humidity and rain amount. Lower panel: Relation between residual concentration (observed – estimated from the regression with OBC) of  $\text{NH}_3 + \Delta \text{NH}_4^+$  and air temperature. All meteorological data were obtained at the meteorological observatory.